Grain size effect in conductive phosphate / carbon nanotube ceramics

Artyom Plyushch[a,*], Polina P. Kuzhir[a], Sergey A. Maksimenko[a], Jan Macutkevič[b], Jūras Banys[b], Aliaksei Sokal[c], Konstantin N. Lapko[c], Vladislav Arkhipov[d], Alexander Okotrub[d]

[a]*Research Institute for Nuclear Problems of Belarusian State University, Bobruiskaya Str. 11, Minsk 220030 Belarus*
[b]*Faculty of Physics, Vilnius University, Sauletekio 9, Vilnius LT-10222, Lithuania*
[c]*Research Institute for Physical Chemical Problems of the Belarusian State University, 14 Leningradskaya Str., Minsk 220030, Belarus*
[d]*Nikolaev Institute of Inorganic Chemistry, SB RAS, 3 Ac. Lavrentyev Ave., 630090 Novosibirsk, Russia*

Abstract

Composite materials based on aluminium phosphate matrix with different grain sizes and small inclusions of carbon nanotubes were studied by means of broadband dielectric spectroscopy in a wide frequency (20 Hz - 36 GHz) and temperature (25-600 K) ranges. The highest electrical percolation threshold was observed for ceramics with the grain size of 0.8 μm, which is higher than the carbon nanotubes cluster size. The electrical transport in ceramics occurs due to the thermal activation at higher temperatures (above room temperature) and the tunneling at lower temperatures. The potential barrier for electron hopping is the lowest in nanosized ceramics. The distance for electron tunneling is also lowest in nanosized ceramics. The electrical properties of ceramics are stable up to 560 K.

Keywords: Composite materials, phosphates, carbon nanotube, dielectric permittivity, grain size

1. Introduction

Design and development of composite materials based on inorganic matrices with carbon **nanoscale** inclusions is one of the most perspective field of modern material science. Although a number of studies **have been** published[1, 2, 3, 4], these inorganic systems have received much less attention than carbon nanotubes/polymer matrix composites (see reviews [5, 6, 7, 8, 9] and Refs there in). The main interest of studying such systems is caused on the one hand **by** the high hardness, good wear resistance, and corrosion resistance of inorganic matrices (like alumina, Al_2O_3) which makes it attractive **from both research and ceramic engineering prospectives** [10]. On the other hand, due to **the** outstanding thermal and electric conductivity, mechanical properties [11] of carbon nanotubes became one

---

*I am corresponding author
  Email address: artyom.plyushch@inp.bsu.by (Artyom Plyushch)

of the most commonly used and investigated. Such enrichment allows to obtain composites with low percolation threshold [12], significantly improved electric and thermal conductivity [13, 14], mechanical properties [15, 16, 17, 18].

The most critical point of development of such types of ceramics – is to find the correlations between the microstructure and macroscopic properties [19, 20]. For instance, functionalization of multi-walled CNT (MWCNT) impacts on conductivity, density, and hardness of alumina / MWCNT ceramics fabricated *via* spark plasma sintering (SPS) [21]. It was demonstrated that the electrical conductivity of SPS alumina-CNT nanocomposite increased with **the growth** grain size. **The effect is** due to **the** increase in the density of CNTs at the grain boundaries [22]. Also different mixing methods and pressing rapidity of MWCNT and Al_2O_3 impacts on mechanical properties such as fracture toughness, flexural strength [16], and thermal conductivity [23].

In our previous works, it was demonstrated that MWCNT's aspect ratio [24], utilization of different binders [25], and chemical modification of nanotubes [26, 27] affects the dielectric permittivity, conductivity, and the mechanical properties of the samples. The aim of this paper is to investigate the impact of the grain size on broadband dielectric properties of composite materials based on aluminium phosphate ceramics with small inclusions (up to 2 *wt.* %) of MWCNT.

2. Methodology and sample preparation

Thermally stable phosphate ceramic based on liquid aluminium phosphate binder and mixture of aluminium nitrate and oxide as a filler was utilized as a composite matrix. Aluminium phosphate binder was prepared by dissolving hydroxide ($Al(OH)_3$) in phosphoric(V) acid (H_3PO_4) with **the** molar ratio of acid to hydroxide equal to 3. The mass ratio of aluminium oxide and aluminium nitrate (average grain size 60 nm, "Plasma & Ceramic Technologies" Ltd., `http://www.plazmaker.lv/products/AlN_PD%20isa_v01.pdf`, grade A) was equal to 9. Alumina utilized for composite preparation was of three different size ranges: with average size 50 nm ("Plasma & Ceramic Technologies" Ltd., `http://www.plazmaker.lv/products/Al2O3_PD%20isa_v01.pdf`, grade B), M1, with median grain size d_{s50} - $0.8 \pm 0.2 \mu m$ and M10, FEPA F800, with median grain size d_{s50} - $6.5 \pm 1.0 \mu m$ RUSAL, Russia, `http://www.rusal.ru/en/clients/products/korund_products/`. Further in the text, they will be referred as Nano, M1, and M10, correspondingly.

As a functional filler multiwall carbon nanotubes (MWCNT) grown by catalytic chemical vapor deposition method [28] were used. Synthesis was performed with CVD-reactor on the quartz plates with 200x300 mm in dimensions. **The** synthesis procedure consists of: blowing the reaction camera with nitrogen to remove the O_2, heating up to 1043 K and blowing camera with the mixture of nitrogen (90 ml/s), toluene (16 ml/s), and ferrocene (7 % of toluene mass) during 15 min. After synthesis camera was blown with nitrogen to remove side-products of reaction and reagents and cooled down to the room temperature. As a results arrays of MWCNTs with **the** diameter of 50 nm and length of 100 μm oriented perpendicularly to **the** substrate were produced (fig. 1). Arrays were mechanically removed from the substrate and milled with the mixer. As-produced MWCNT contains $\alpha - Fe$ parti-

cles encapsulated into the hollows of CNTs (4 $wt.$ %) and almost doesn't contain amorphous carbon.
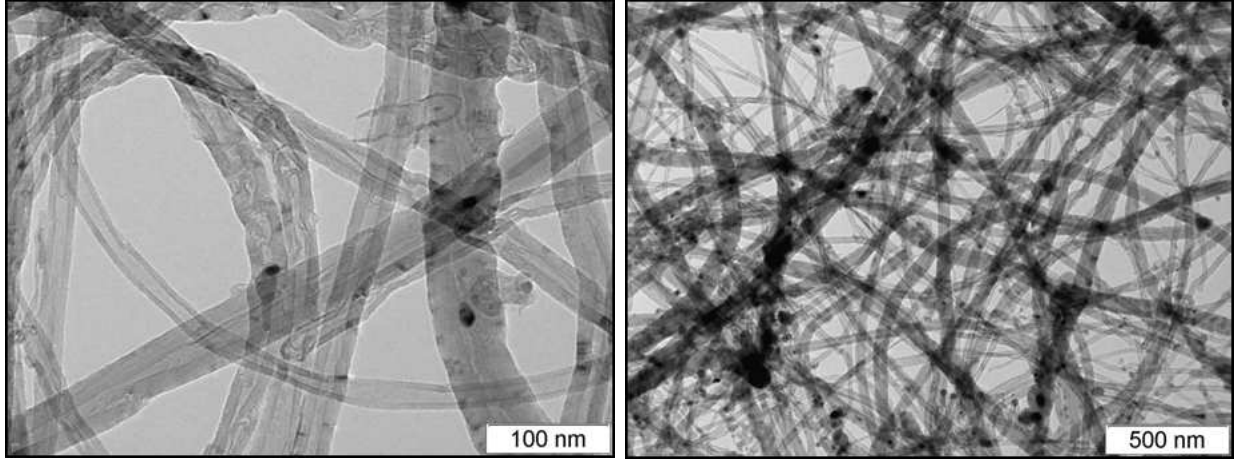
Figure 1: TEM images of as-obtained MWCNT

Composite preparation procedure as follows. MWCNTs, Al_2O_3 filler and aluminum-phosphate binder have been ground for $20 - 30$ min in an agate mortar until obtaining a homogeneous mixture. Then the mixture was pressed under 4.9 MPa in 1 mm thick tablets of 10 mm diameter. After 24 h of treatment at room temperature, the tablets were treated at temperatures up to 300 $°C$, with a rate of 1 $°C min^{-1}$. Three series of composites with different grain sizes and MWCNT concentrations of 0, 0.2, 0.5, 1, 1.5 and 2 $wt.$ % have been prepared (see fig. 2)
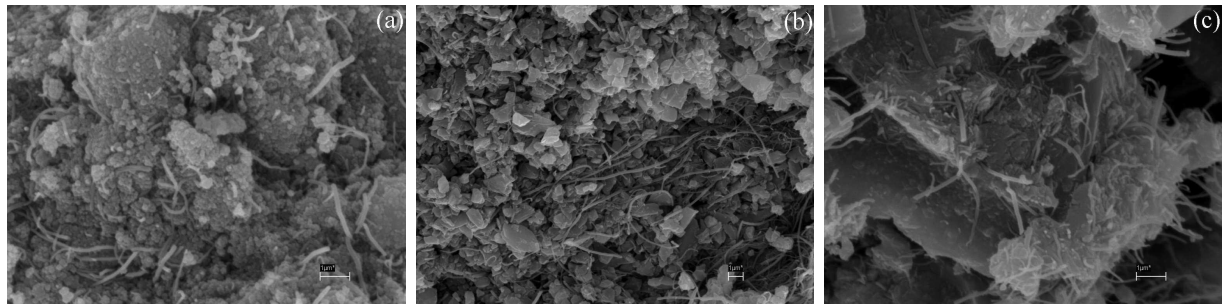
Figure 2: Scanning electron microscopy of composite materials with 2 $wt.$ % of MWCNT: Nano (a), M1 (b), M10 (c)

In the frequency range 20 Hz-1 MHz dielectric properties were measured with a LCR HP4284A meter. Two equivalent schemes ($Cp - D$ and $R - X$) were used for measurements. For low temperature measurements (25-300 K) samples were placed in the closed cycle cryostat, while for high temperature (300 - 500 K) measurements a home-made furnace was used. The square-like samples with **the** typical thickness about 1 mm and area of 30 mm^2 were investigated. Silver paste was applied for contacting.

In the frequency range 1 MHz-3 GHz measurements were performed by a coaxial dielectric spectrometer with vector network analyzer Agilent 8714ET. Sample with **the** typical area of 2 mm^2 and thickness of 0.7 mm were studied. Silver paste was applied for contacting.

The microwave measurements were carried out with a scalar network analyzer R2-408R (ELMIKA, Vilnius, Lithuania). Rod-like samples with typical diameter $d = 0.4$ mm were studied. The EM responses of samples were measured within the 26-37 GHz frequency range (Ka-band) as ratios of transmitted/**incident** (S_{21})and reflected/**incident** (S_{11}) signals. The conductivity was reconstructed from **the** S-parameters *via* methods described **in** [29].

3. Results and discussion

3.1. Room temperature region

The dielectric analysis of ceramics demonstrated, that ceramics without MWCNT has exactly the same properties for all **of the grain sizes** investigated. **No DC conductivity plateau is seen in conductivity spectra while the value of 10 nS/m of AC conductivity is observed at 129 Hz for all investigated grain sizes.** The addition of nanotubes **extensively increases the** ceramic conductivity (15 S/m for 2 $wt.$ % of MWCNT in M10 matrix) in a wide frequency range. However, embedding the same amount of nanotubes into different grain size matrices leads to different effects. Figure 3 (a) represents the typical frequency dependence of the composite's conductivity with the **given** concentration of MWCNT. Samples M10 and Nano at 1 $wt.$ % have the conductivity plateau at low frequencies. That is their frequency dependence can be described **by** the Almond-West power law [30] (fig. 3 (a), solid curves):

$$\sigma = \sigma_{DC} + \sigma_{AC}(\omega) = \sigma_{DC} + A\omega^r \ , \tag{1}$$

where σ_{DC} is the DC conductivity and $A\omega^r$ is the AC conductivity. We can conclude, that the grain size influences the distribution of MWCNT and consequently the conductivity of samples. Indeed, analyzing samples with different concentrations at the fixed frequency (for example 129 Hz (see fig 3 (b), symbols) one observes the huge **spread** (up to 9 orders) in conductivity of samples **for** the given MWCNT concentration. This fact indicates that the percolation threshold depends on the grain size of **studied** samples. In order to obtain the precise values of the percolation threshold the following formula may be applied [31]:

$$\begin{cases} \sigma = \sigma_0 (\frac{p_{CNT} - p_c}{p_c})^{-s}, & p_{CNT} < p_c \ , \\ \sigma = \sigma_i (\frac{p_c - p_{CNT}}{p_c})^{t}, & p_{CNT} > p_c \ , \end{cases} \tag{2}$$

where σ_0 is the matrix conductivity, σ_i is the inclusions conductivity, s and t **are** the critical exponents. Analyzing the concentration behaviour of the conductivity for M1 samples with first eq. of (2) and M10 and Nano with both eq. of (2) (see fig. 3 (b), solid curves) we come to the parameters presented in Table.1.

4
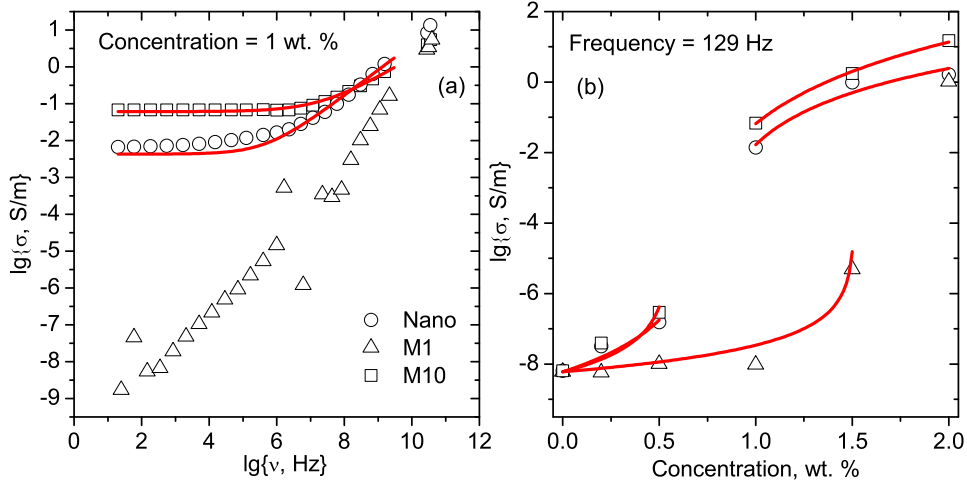
Figure 3: Frequency dependence of the conductivity for samples with 1 wt. % of MWCNT (a); concentration dependence of the conductivity of composite material with different amount of MWCNT (b)

Table 1: **Parameters of fits with equations 2**

Sample series	M10	M1	Nano
p_c, wt. %	0.56	1.52	0.75
s	1.84	1.61	3.14
$lg\{\sigma_0, S/m\}$	-8.22	-8.22	-8.22
t	4.52	—	3.12
$lg\{\sigma_i, S/m\}$	0.18	—	0.48

It is known that, the dependence of macroscopic properties (i.e. the conductivity, the percolation threshold, the effective permittivity) of such type of composites (CNTs/ceramics) should be a monotonically dependent on the micro structure of composites, in our case with **the** variation of the grain size [19]. Since nanotubes can be located only in grain boundary area, we may conclude, that with **the** increase of the grain size the grain boundary area decreases, and **hence** the density of CNTs at the grain boundaries increases [22]. Therefore, if CNTs are randomly distributed, the **average** distance between CNTs and the percolation threshold **value** is lower in ceramics with bigger grains.

This can be considered more strictly: for example, a model of two types of grains of the irregular shape mixed together with R_1 and R_2 – effective radii of non-conductive and conductive grains, correspondingly, predicts the monotonous decreasing of the percolation threshold with R_1/R_2 increasing [19]. Of course, in **the** case of nanotube/ceramics composites it is not pretty correct to assign CNTs as a grain with irregular shape, however, aggregates of nanotubes can be considered as ones. In the case of Nano-sized grains ceramics, the size of nanotubes is comparable with the mean value of the grain's effective radius. It can be expected that during preparation the part of CNT's aggregates may be destroyed. As a result, the aggregates of MWCNT in Nano-composites should be smaller than one

5

for M1 and M10. Much more for Nano-sized grain ceramics it would be possible that the tunnelling of electrons through insulating grain matrix, also **participate in the** increase **of** the total conductivity of the samples. This means, that p_c as a function of (R_{eff}) (where R_{eff} is an effective alumina grain radius) should have the maximum for grains, which size is close to the CNTs cluster size.

3.2. High temperature region

Results of thermogravimetric analysis of composite materials are presented in fig. 4 The
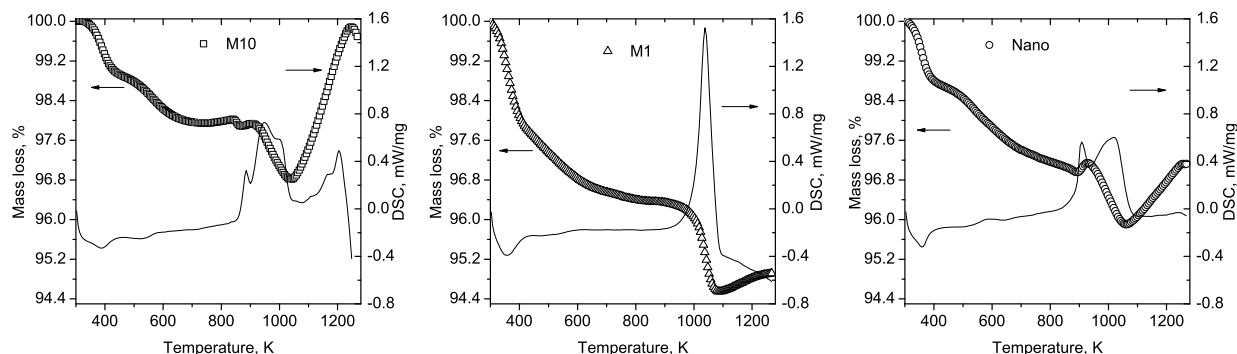
Figure 4: Thermogravimetric analysis of composite materials with 2 *wt.* % of MWCNT

DSC curve demonstrates two thermal effects in temperature ranges 290-470 K and 870-1270 K. The endothermic effect close to 373 K have the weight loss of 2 % and it is related **to** the evaporation of water. **The presence of water inside the samples may be attributed to the water absorbed from the atmosphere and the one appearing during reactions of binder and filler, and polycondensation reactions.** In temperature range 470-870 K some polycondensation reactions take place. The corresponding weight loss of 2% is observed in this range. However, these reactions do not demonstrate any DSC effect. The exothermic effects in temperature range 870-1270 K are related with the thermal-oxidative destruction of MWCNTs.

Composite materials with non-zero DC-conductivity have been studied at higher temperatures (above the room temperature). As we can see from the measurement results (Fig. 5, symbols), the relative **increase** of the conductivity of M10-series samples is higher than for Nano-samples **of** all studied concentration. M1 2 *wt.* % sample demonstrates even the higher thermal stability than M10- and Nano-. The **increase** of the conductivity during heating governs the Arrhenius law:

$$\sigma_{DC} = \sigma_0 e^{-\frac{E_a}{kT}} , \tag{3}$$

where E_a is the activation energy. The Arrhenius fit parameters are presented in Table 2. It is important to note that the neat ceramics DC conductivity is strictly zero. Therefore, the electrical transport in ceramics occurs mainly due to the electron tunneling between CNT's clusters. Much more the conductivity activation energy is lower in Nano-samples

Table 2: Activation energies

Series; p, $wt.\%$	M10; 2	M10; 1.5	M10; 1	M1; 2	Nano; 2	Nano; 1.5	Nano; 1
E_a/k, K	516.68	486.78	684.16	341.87	412.42	325.83	421.47
E_a, meV	**44.54**	**41.96**	**58.97**	**29.47**	**35.55**	**28.09**	**36.33**

(see Table. 2). **However, the concentration dependence of the activation energy is less observed, mainly due to the fact that all samples are far from percolation threshold [32].** At higher temperatures, there exists a peak of conductivity with its maximum at temperature of 600-620 K. This peak may be related to polycondensation reactions.
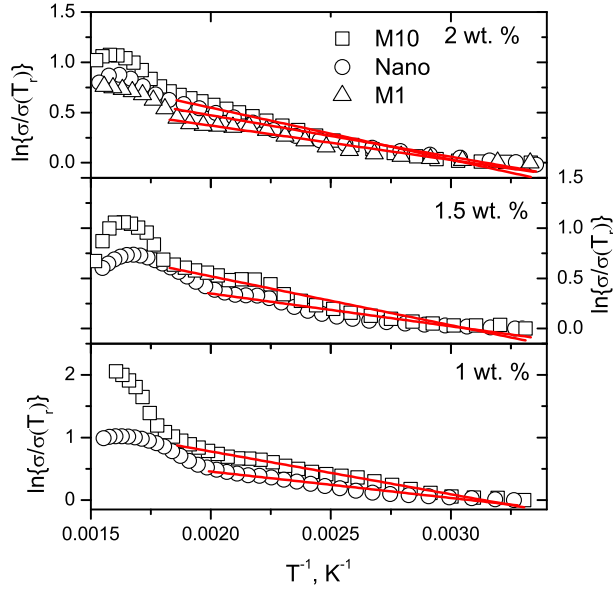
Figure 5: Temperature dependence of the relative DC-conductivity for samples with the different concentration of carbon nanotubes.

3.3. Low temperature region

The temperature behaviour of the DC-conductivity of percolated samples was studied on cooling down to 25 K (see Fig. 6, symbols). As we can see from figure 6, the conductivity decreases during cooling cycle down to 60-70% of it's initial value. The conductivity of composites with Nano grains demonstrate better thermal stability for all studied MWCNT concentrations (for instance, samples with 2 wt.% with Nano matrix loose only 15% of the initial value, while M10 and M1 loose 30%). At lower concentrations this difference becomes negligible. However, for all studied MWCNT concentrations Nano samples demonstrate the smaller decrease of the conductivity than M10. The variation of the conductivity for all samples can be well described **by** tunneling law [33] (Fig. 6, solid curve line):

$$\sigma_{DC} = \sigma_0 e^{-\frac{T_1}{T+T_0}}, \tag{4}$$

7
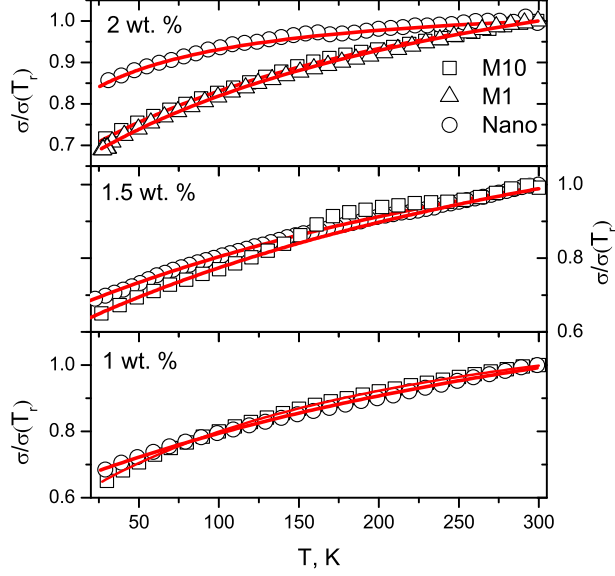
Figure 6: Temperature dependence of the relative DC-conductivity for samples with **the** different concentration of carbon nanotubes.

Table 3: Parameters of the tunneling law fit

Series; p, $wt.\%$	M10; 2	M10; 1.5	M10; 1	M1; 2	Nano; 2	Nano; 1.5	Nano; 1
T_1	128.87	266.76	121.85	137.04	23.02	255.6	276.31
T_0	186.44	277.0	145.74	183.59	73.1	300.88	307.85
T_1 / T_0	0.691	0.963	0.836	0.746	0.315	0.849	0.898

where T_1 represents the energy required for an electron to cross the insulator gap between conductive particle aggregate, and T_0 is the temperature above which the thermally activated conduction over the barriers begins to occur. Values of T_1 and T_0 utilized for fit are collected in Table 3

According to the tunneling law, values of T_1 and T_0 are related **to** conductive cluster distribution according to following equations[33]:

$$T_1 = \frac{U\epsilon_0^2}{k} \tag{5}$$

$$T_0 = \frac{2U\epsilon_0^2}{\pi\chi\omega k} = \frac{2T_1}{\pi\chi\omega} \tag{6}$$

In these expressions, $U = \omega A/8\pi$ is a measure of the volume of the tunnel junction, $\epsilon_0 = 4V_0/e\omega$ is a pre-exponential factor, $\chi = \sqrt{2m_e V_0/\hbar}$ is the tunneling constant for electrons, where V_0 is the potential barrier, A and ω **are the area and the thickness of the insulating gap between conductive clusters respectively**. According to eqs. 5 and 6, $T_1/T_0 = \pi\chi\omega/2 = (\pi/2)\sqrt{2m_e/\hbar} \ V_0^{1/2}\omega$. As it can be seen from table 3 **the**

8

increase in the concentration leads to the decrease the value T_1/T_0 for Nano ceramics. This is equivalent to the decrease of the potential barrier V_0 and/or the separation distance ω between conductive clusters when the nanotube's concentration increase. On the other hand, composites with smallest grains (Nano) have the lower value of T_1/T_0 than M10 composites (with except of 1 $wt.$ % sample).

It is important to note that at higher temperatures (T>>T$_0$) the tunneling law (eqs. 4) becomes the Arrhenius law (eqs. 3) and the activation energy in the Arrhenius law should be equal to T$_1$. However, the activation energy values presented in Table 2 are higher than the values of T$_1$ presented in Table 3. It indicates that above the room temperature additional effects (like thermally activated electron hopping) affect the total electrical conductivity.

We can conclude, that due to the different distribution of nanotubes, the tunnelling potential barrier and the separation of composites **varies** significantly. The samples with **Nano** grains demonstrate better tunnelling abilities than the samples based on microsized - grains ceramics.

4. Conclusions

Clearing out the relations between microstructure and macroscopic properties of composite materials is one of the critical **points** in material science. The influence of the mean grain size of the ceramic matrix **has** been studied on broadband electrical properties at different temperatures. It was demonstrated, that the percolation threshold has non-monotonous dependence on the mean grain size with **the** maximum of the percolation concentration observed for composites with M1 (d_{s50} - $0.8 \pm 0.2 \mu m$) grains. High temperature analysis demonstrates that conductivity activation energy is the highest for M10 (d_{s50} - $6.5 \pm 1.0 \mu m$) grains.

5. Acknowledgements

References

[1] J. Cho, A. R. Boccaccini, M. S. Shaffer, Ceramic matrix composites containing carbon nanotubes, Journal of Materials Science 44 (8) (2009) 1934–1951.

[2] S. S. Samal, S. Bal, et al., Carbon nanotube reinforced ceramic matrix composites-a review, Journal of Minerals and Materials Characterization and Engineering 7 (04) (2008) 355.

[3] G.-D. Zhan, J. D. Kuntz, J. Wan, A. K. Mukherjee, Single-wall carbon nanotubes as attractive toughening agents in alumina-based nanocomposites, Nature materials 2 (1) (2003) 38–42.

[4] X. Wang, N. P. Padture, H. Tanaka, Contact-damage-resistant ceramic/single-wall carbon nanotubes and ceramic/graphite composites, Nature materials 3 (8) (2004) 539–544.

[5] J. N. Coleman, U. Khan, W. J. Blau, Y. K. Gunko, Small but strong: a review of the mechanical properties of carbon nanotube–polymer composites, Carbon 44 (9) (2006) 1624–1652.

[6] W. Bauhofer, J. Z. Kovacs, A review and analysis of electrical percolation in carbon nanotube polymer composites, Composites Science and Technology 69 (10) (2009) 1486–1498.

[7] P.-C. Ma, N. A. Siddiqui, G. Marom, J.-K. Kim, Dispersion and functionalization of carbon nanotubes for polymer-based nanocomposites: a review, Composites Part A: Applied Science and Manufacturing 41 (10) (2010) 1345–1367.

[8] M. H. Al-Saleh, U. Sundararaj, A review of vapor grown carbon nanofiber/polymer conductive composites, Carbon 47 (1) (2009) 2–22.

[9] M. Rahmat, P. Hubert, Carbon nanotube–polymer interactions in nanocomposites: a review, Composites Science and Technology 72 (1) (2011) 72–84.

[10] W. Wang, G. Yamamoto, K. Shirasu, Y. Nozaka, T. Hashida, Effects of processing conditions on microstructure, electrical conductivity and mechanical properties of mwcnt/alumina composites prepared by flocculation, Journal of the European Ceramic Society 35 (14) (2015) 3903–3908.

[11] M. M. J. Treacy, T. W. Ebbesen, J. M. Gibson, Exceptionally high young's modulus observed for individual carbon nanotubes, Nature 381 (6584) (1996) 678–680.
URL http://dx.doi.org/10.1038/381678a0

[12] S. Rul, F. Lefevre-Schlick, E. Capria, C. Laurent, A. Peigney, Percolation of single-walled carbon nanotubes in ceramic matrix nanocomposites, Acta Materialia 52 (4) (2004) 1061–1067.

[13] G.-D. Zhan, J. D. Kuntz, J. E. Garay, A. K. Mukherjee, Electrical properties of nanoceramics reinforced with ropes of single-walled carbon nanotubes, Applied Physics Letters 83 (6) (2003) 1228–1230.

[14] G.-D. Zhan, A. K. Mukherjee, Carbon nanotube reinforced alumina-based ceramics with novel mechanical, electrical, and thermal properties, International Journal of Applied Ceramic Technology 1 (2) (2004) 161–171.

[15] M. Mazaheri, D. Mari, Z. R. Hesabi, R. Schaller, G. Fantozzi, Multi-walled carbon nanotube/nanostructured zirconia composites: Outstanding mechanical properties in a wide range of temperature, Composites Science and Technology 71 (7) (2011) 939–945.

[16] S. Bi, G. Hou, X. Su, Y. Zhang, F. Guo, Mechanical properties and oxidation resistance of α-alumina/multi-walled carbon nanotube composite ceramics, Materials Science and Engineering: A 528 (3) (2011) 1596–1601.

[17] M. Estili, A. Kawasaki, H. Sakamoto, Y. Mekuchi, M. Kuno, T. Tsukada, The homogeneous dispersion of surfactantless, slightly disordered, crystalline, multiwalled carbon nanotubes in α-alumina ceramics for structural reinforcement, Acta Materialia 56 (15) (2008) 4070–4079.

[18] B. Yazdani, Y. Xia, I. Ahmad, Y. Zhu, Graphene and carbon nanotube (gnt)-reinforced alumina nanocomposites, Journal of the European Ceramic Society 35 (1) (2015) 179–186.

[19] C.-W. Nan, Physics of inhomogeneous inorganic materials, Progress in Materials Science 37 (1) (1993) 1–116.

[20] G. Yamamoto, K. Shirasu, Y. Nozaka, W. Wang, T. Hashida, Microstructure–property relationships in pressureless-sintered carbon nanotube/alumina composites, Materials Science and Engineering: A 617 (2014) 179–186.

[21] A. C. Zaman, C. B. Üstündağ, F. Kaya, C. Kaya, Oh and cooh functionalized single walled carbon nanotubes-reinforced alumina ceramic nanocomposites, Ceramics International 38 (2) (2012) 1287–1293.

[22] F. Inam, H. Yan, D. D. Jayaseelan, T. Peijs, M. J. Reece, Electrically conductive alumina–carbon nanocomposites prepared by spark plasma sintering, Journal of the European Ceramic Society 30 (2) (2010) 153–157.

[23] O. Hanzel, J. Sedláček, E. Hadzimová, P. Šajgalík, Thermal properties of alumina–mwcnts composites, Journal of the European Ceramic Society 35 (5) (2015) 1559–1567.

[24] A. Plyushch, D. Bychanok, P. Kuzhir, S. Maksimenko, K. Lapko, A. Sokol, J. Macutkevic, J. Banys, F. Micciulla, A. Cataldo, S. Bellucci, Heat-resistant unfired phosphate ceramics with carbon nanotubes for electromagnetic application, physica status solidi (a) 211 (11) (2014) 2580–2585. doi:10.1002/pssa.201431306.

[25] N. Apanasevich, A. Sokal, K. Lapko, A. Kudlash, V. Lomonosov, A. Plyushch, P. Kuzhir, J. Macutkevic, J. Banys, A. Okotrub, Phosphate ceramics / carbon nanotubes composites:liquid aluminum phosphate vs solid magnesium phosphate binder, Ceramics International 41 (9, Part B) (2015) 12147 – 12152.

doi:http://dx.doi.org/10.1016/j.ceramint.2015.06.033.

[26] M. A. Kanygin, O. V. Sedelnikova, I. P. Asanov, L. G. Bulusheva, A. V. Okotrub, P. P. Kuzhir, A. O. Plyushch, S. A. Maksimenko, K. N. Lapko, A. A. Sokol, O. A. Ivashkevich, P. Lambin, Effect of nitrogen doping on the electromagnetic properties of carbon nanotube-based composites, Journal of Applied Physics 113 (14). doi:http://dx.doi.org/10.1063/1.4800897.

[27] A. O. Plyushch, A. A. Sokol, K. N. Lapko, P. P. Kuzhir, Y. V. Fedoseeva, A. I. Romanenko, O. B. Anikeeva, L. G. Bulusheva, A. V. Okotrub, Electromagnetic properties of phosphate composite materials with boron-containing carbon nanotubes, Physics of the Solid State 56 (12) (2014) 2537–2542. doi:10.1134/S1063783414120257.

[28] A. V. Okotrub, L. G. Bulusheva, A. G. Kudashov, V. V. Belavin, S. V. Komogortsev, Arrays of carbon nanotubes aligned perpendicular to the substrate surface: Anisotropy of structure and properties, Nanotechnologies in Russia 3 (3) (2008) 191–200. doi:10.1134/S1995078008030051.

[29] E. Nielsen, Scattering by a cylindrical post of complex permittivity in a waveguide, Microwave Theory and Techniques, IEEE Transactions on 17 (3) (1969) 148–153. doi:10.1109/TMTT.1969.1126913.

[30] D. Almond, G. Duncan, A. West, The determination of hopping rates and carrier concentrations in ionic conductors by a new analysis of ac conductivity, Solid State Ionics 8 (2) (1983) 159–164. doi:10.1016/0167-2738(83)90079-6.

[31] E. J. Garboczi, K. A. Snyder, J. F. Douglas, M. F. Thorpe, Geometrical percolation threshold of overlapping ellipsoids, Phys. Rev. E 52 (1995) 819–828. doi:10.1103/PhysRevE.52.819.

[32] J. Macutkevic, P. P. Kuzhir, A. G. Paddubskaya, J. Banys, S. A. Maksimenko, E. Stefanutti, F. Micciulla, S. Bellucci, Broadband dielectric/electric properties of epoxy thin films filled with multiwalled carbon nanotubes, Journal of Nanophotonics 7 (1) (2013) 073593–073593. doi:10.1117/1.JNP.7.073593

[33] P. Sheng, E. K. Sichel, J. I. Gittleman, Fluctuation-induced tunneling conduction in carbon-polyvinylchloride composites, Phys. Rev. Lett. 40 (1978) 1197–1200. doi:10.1103/PhysRevLett.40.1197.